GEOSTANDARDS and GEOANALYTICAL RESEARCH

High-Precision Mass-Dependent Molybdenum Isotope Variations in Magmatic Rocks Determined by Double-Spike MC-ICP-MS

Matthias **Willbold** (1, 2)*, Kate **Hibbert** (2), Yi-Jen **Lai** (2, 3), Heye **Freymuth** (2), Remco C. **Hin** (2), Christopher **Coath** (2), Flurin **Vils** (2) and Tim **Elliott** (2)

(1) School of Earth, Atmospheric and Environmental Sciences, University of Manchester, Williamson Building, Oxford Road, Manchester, M13 9PL, UK
(2) School of Earth Sciences, University of Bristol, Wills Memorial Building, Queens Road, Bristol, BS8 1RJ, UK
(3) ETH Zürich, Institute of Geochemistry and Petrology, NW D85, Clausiusstrasse 25, 8092 Zürich, Switzerland
* Corresponding author. e-mail: matthias.willbold@manchester.ac.uk

Small mass-dependent variations of molybdenum isotope ratios in oceanic and island arc rocks are expected as a result of recycling altered oceanic crust and sediments into the mantle at convergent plate margins over geological timescales. However, the determination of molybdenum isotope data precise and accurate enough to identify these subtle isotopic differences remains challenging. Large sample sizes – in excess of 200 mg – need to be chemically processed to isolate enough molybdenum in order to allow sufficiently high-precision isotope analyses using double-spike MC-ICP-MS techniques. Established methods are either unable to process such large amounts of silicate material or require several distinct chemical processing steps, making the analyses very time-consuming. Here, we present a new and efficient single-pass chromatographic exchange technique for the chemical isolation of molybdenum from silicate and metal matrices. To test our new method, we analysed USGS reference materials BHVO-2 and BIR-1. Our new data are consistent with those derived from more involved and time-consuming methods for these two reference materials previously published. We also provide the first molybdenum isotope data for USGS reference materials AGV-2, the GSJ reference material JB-2 as well as metal NIST SRM 361.

Keywords: molybdenum, Mo, mass-dependent, stable isotopes, oceanic basalts, mantle recycling, anionic chromatographic exchange, double spike, MC-ICP-MS.

Les petites variations des rapports isotopiques de Mo dépendant de masse dans les roches océaniques et les arcs insulaires résultent du recyclage de la croûte océanique alterée et les sédiments dans le manteau à des marges de plaques convergentes à des échelles de temps géologiques. Toutefois, la détermination des données d'isotopes de molybdène suffisamment précis pour identifier ces différences isotopiques subtiles reste difficile. Échantillons de grandes tailles - de plus de 200 mg - doivent être traitées chimiquement pour isoler suffisamment de molybdène afin de permettre les analyses de suffisamment de haute précision utilisant MC-ICP-MS par la méthode du 'double-spike'. Les méthodes établies sont soit incapable de traiter de telles quantités de silicate ou nécessitent plusieurs étapes distinctes de traitement chimique, ce qui rend l'analyse très lent. Ici, nous présentons une nouvelle technique d'échange chromatographique à isoler le Mo à partir de silicates et métaux. Pour tester notre nouvelle méthode, nous avons analysé les matériaux de référence USGS BHVO-2 et BIR-1. Nos nouvelles données sont compatibles avec ceux issus de méthodes plus complexes pour ces deux matériaux de référence publiés antérieurement. Nous fournissons également les premières données sur les isotopes de molybdène pour les matériaux de référence USGS AGV-2, GSJ JB-2 et NIST SRM 361.

Mots-clés : Molybdène, Mo, isotopes stables, dépendant de masse, basaltes océaniques, recyclage manteau, échange chromatographique anionique, double-spike, MC-ICP-MS.

Received 04 Aug 15 – Accepted 26 Nov 15

doi: 10.1111/ggr.12109

Mass-dependent variations of molybdenum (Mo) isotopes in marine sediments are a well-established geochemical tool to study redox conditions in the Earth's water masses over the geological past (e.g., Barling *et al.* 2001, Siebert *et al.* 2003, Archer and Vance 2008). During surface processing, the speciation and thus solubility of Mo in aqueous systems strongly depend on the ambient redox conditions (e.g., Emerson and Huested 1991, Helz *et al.* 1996). This makes the Mo isotope system highly susceptible to natural mass-dependent isotope fractionation (McManus *et al.* 2002, Barling and Anbar 2004, Wasylenki *et al.* 2008). As a consequence, sedimentary rocks can show mass-dependent $^{98}Mo/^{95}Mo$ isotope variations of up to 5‰ (e.g., Siebert *et al.* 2003, Anbar 2004, Pearce *et al.* 2008, Gordon *et al.* 2009, Scheiderich *et al.* 2010b). Similarly, exchange reactions between the seafloor and the hydrosphere are likely to impart Mo isotope variations on altered mafic and ultramafic oceanic rocks due to the rather large isotopic difference of *ca.* 2.5‰ between seawater and fresh oceanic crust (e.g., Anbar 2004). Thus, the $^{98}Mo/^{95}Mo$ of mantle-derived rocks from subduction zones and ocean island basalts could be useful to trace crustal material recycled into the Earth's mantle.

Although the $^{98}Mo/^{95}Mo$ of the uppermost oceanic crust can be significantly perturbed, the bulk of recycled component, dominantly comprising mafic lithologies that have been little altered, is likely to carry a much less fractionated signal. Thus, only small isotopic perturbations are expected for oceanic mantle-derived rocks containing such a recycled component. In fact, the total variation in $^{98}Mo/^{95}Mo$ of magmatic rocks from various tectonic settings analysed so far is less than 1‰ (Siebert *et al.* 2003, Pearce *et al.* 2009, Burkhardt *et al.* 2014, Greber *et al.* 2014, Voegelin *et al.* 2014, Freymuth *et al.* 2015, Greber *et al.* 2015, Yang *et al.* 2015). To resolve and understand such subtle isotopic variations, high-precision Mo isotope data for magmatic rocks are required. Mo isotope data with low measurement uncertainties can be achieved using multi-collector inductively coupled plasma-mass spectrometry (MC-ICP-MS) combined with a double-spike method (Siebert *et al.* 2001, Archer and Vance 2008, Pearce *et al.* 2009). This method allows robust correction of instrument-induced isotopic fractionation in natural samples (e.g., see Rudge *et al.* 2009).

Complications arise from the low concentration of Mo in mantle-derived melts when compared to chemical sediments on which most Mo isotope work to date has been conducted (see Anbar 2004). Even when using sensitive mass spectrometric techniques, such as MC-ICP-MS, sufficient amounts of Mo in the order of ~ 100 ng of Mo per analysis are needed to obtain the levels of precision required for geologically relevant observations in mantle-derived samples. The low Mo concentrations in many mafic rocks, a few hundred ng g^{-1} in mid-ocean ridge basalts (MORB), for example, means that large sample sizes (up to grams) have to be subjected to a chemical purification procedure. Previous single-column pass Mo separation techniques were designed to process small sample sizes (< 0.1 g) and are perfectly suitable for the analyses of Mo-rich sediments (e.g., Archer and Vance 2008, Goldberg *et al.* 2012, Xu *et al.* 2012). However, these methods may struggle to cope with the large sample loads required when processing mafic magmatic rocks. One way of overcoming this obstacle is to simply scale up existing protocols by increasing the volumes of chromatographic exchange resins and mobile phases (i.e., mineral acids). However, anionic chromatographic exchange resins are a major source of Mo blank. Therefore, increasing the volume of resin is not ideal from considerations of blank contribution or processing time. Alternatively, several procedures employing solvent extraction as well as multiple passes on high-volume cationic and anionic resin columns have been developed (Dauphas *et al.* 2001, Yin *et al.* 2002, Becker and Walker 2003, Wille *et al.* 2007, Burkhardt *et al.* 2014, Nagai and Yokoyama 2014). These methods achieve isolation of Mo through stepwise reduction of matrix elements and may tolerate higher sample loads. They are, however, very time-consuming and still require large resin volumes. The lack of a more efficient and convenient chemical separation technique therefore remains one of the main obstacles in undertaking a comprehensive study of Mo mantle isotope systematics. In fact, there are few Mo isotope data available for magmatic rocks (Siebert *et al.* 2003, Pearce *et al.* 2009, Burkhardt *et al.* 2014, Greber *et al.* 2014, Voegelin *et al.* 2014, Greber *et al.* 2015, Yang *et al.* 2015). This is also expressed in a lack of Mo isotope data for well-characterised magmatic geological reference materials.

This study reports on the development of a new, low-volume, single-pass anion exchange separation technique that allows quantitative isolation of Mo from a range of silicate and metal matrices. At the same time, it can cope with large sample amounts while maintaining low blank levels and processing times. We tested the efficiency and applicability of this new technique by analysing a range of silicate and metal reference materials. The method described will allow efficient processing of mantle-derived rocks and will therefore contribute to establishing mass-dependent Mo isotope variations in magmatic rocks as a geodynamic tracer for geochemical applications.

Chemical preparation procedure

Molybdenum isotope measurements of this study were carried out using MC-ICP-MS. This technique is highly susceptible to interfering elements and polyatomic ions. In particular, several elemental isobaric interferences exist for the seven stable isotopes of Mo (^{92}Mo, ^{94}Mo, ^{95}Mo, ^{96}Mo, ^{97}Mo, ^{98}Mo, ^{100}Mo), namely those of ^{92}Zr, ^{94}Zr, ^{96}Zr, ^{96}Ru, ^{98}Ru and ^{100}Ru. Accordingly, the abundances of matrix elements and especially Zr and Ru need to be reduced to insignificant levels prior to mass spectrometric analysis. The double-spiking scheme we apply uses Mo isotopes that are not interfered by Zr. However, a procedure that separates both Zr and Ru from Mo is advantageous to allow flexibility in the range of double-spikes that can be used, to remove any negative impact of matrix elements on the sensitivity and to permit its use for mass-independent isotopic measurements.

Reagents

Ultrapure grade (UpA) concentrated hydrofluoric acid (28 mol l^{-1}) and hydrogen peroxide (30% *m/m*), as well as super-pure grade (SpA) concentrated nitric acid (15 mol l^{-1}) were purchased from Romil Ltd. Concentrated HCl was purified twice in-house by sub-boiling distillation from analytical grade HCl (final molarity ~ 11 mol l^{-1}). For some samples, Romil Ltd. super-pure grade (SpA) concentrated hydrochloric acid (11–12 mol l^{-1}) was used. ACS-grade (99 + %) ascorbic acid was purchased from Alfa Aesar Ltd.

Dissolution of silicate samples

About 0.1–1.0 g of rock powder and a combined ^{97}Mo–^{100}Mo tracer (in 0.4 mol l^{-1} HNO_3 with traces of HF) were weighed into 15-ml or 60-ml PFA beakers (Savillex Corp.) depending on the sample size. Details concerning the preparation and composition of the combined ^{97}Mo–^{100}Mo tracer can be found in Archer and Vance (2008). For each 0.1 g of sample, about 0.1 ml of 15 mol l^{-1} HNO_3 and 0.3 ml of 28 mol l^{-1} HF were added and samples were digested for at least 24 hrs in closed beakers at *ca.* 150 °C. Samples were then dried down to incipient dryness. The residue was repeatedly dissolved in 6 mol l^{-1} HCl until a clear solution was obtained. Normally, less than two to three cycles of refluxing in HCl were required. We found that this step was necessary to ensure complete removal of fluorides.

Dissolution of metal samples

About 0.01 g of the steel reference material NIST SRM 361 was spiked with the ^{97}Mo–^{100}Mo tracer and dissolved in *ca.* 1 ml of 12 mol l^{-1} HCl at 150 °C overnight. The solutions were visually inspected to ensure complete dissolution. In some cases, dark sub-mm-sized flakes were observed. We assume that these particles represent graphite or iron carbides from the production process of the steel. After drying down the solution, the residue was re-dissolved in 1 ml of 15 mol l^{-1} HNO_3 and heated to 150 °C for several hours to ensure that any flakes were fully oxidised and removed. The samples were then dried down at 150 °C. This step was repeated until a clear solution was obtained. The residues were then converted into chloride form by refluxing in 0.5 ml of 12 mol l^{-1} HCl.

Chemical isolation of molybdenum

Molybdenum was extracted from the silicate and metal matrices of the samples by ion exchange chromatography using the strongly anionic exchange resin AG1x8 (100–200 mesh; BioRad and Eichrom) with various acidic eluents. Before loading on the columns, the samples were brought into solution in a mixture of HCl and ascorbic acid. For *ca.* 200 mg of (basaltic) sample, the residue was dissolved in a mix of 4.50 ml 3 mol l^{-1} HCl and 0.25 ml 6 mol l^{-1} HCl at moderate temperatures (< 150 °C) on a hot plate. The solution was transferred into 10-ml centrifuge vials and centrifuged to remove any precipitates that may have formed during the dissolution of the sample in the dilute HCl loading solution, but which were not visible by the naked eye. Then, 0.25 ml of an aqueous 1 mol l^{-1} ascorbic acid ($C_6H_8O_6$) solution was added. This step was normally accompanied by a change in colour from yellow (Fe^{3+} in HCl solution) to green/colourless (Fe^{2+}) depending on the total iron content of the sample. This yielded a final loading solution of 3 mol l^{-1} HCl – 0.05 mol l^{-1} ascorbic acid. If larger sample sizes or Fe-rich samples were processed (e.g., NIST SRM 361), the relative proportions of 3 mol l^{-1} HCl, 6 mol l^{-1} HCl and 1 mol l^{-1} ascorbic acid solutions were adjusted accordingly. Separate addition of 6 mol l^{-1} and 3 mol l^{-1} HCl to the sample is not necessarily required but facilitates this adjustment.

This sample solution was loaded onto a resin bed of 1 ml of AG1x8 (100–200 mesh) in a column prepared from PTFE shrink tubing with 0.4 cm inner diameter (*ca.* 8-cm resin bed height), which was pre-cleaned and pre-conditioned (Table 1). The bulk of matrix elements (most major elements, rare earth elements) were eluted in 3 mol l^{-1} HCl, followed by rinsing with 0.5 mol l^{-1} HCl – 0.5% *m/m* H_2O_2. The latter removed any remaining trace elements from the resin, most notably Ta, U, Pb and Zn, before Mo was quantitatively eluted in 2 mol l^{-1} HNO_3 (procedure 1). The

Table 1.
Separation procedure 1 on strongly anionic exchange resin (Bio-Rad AG 1x8, 100 –200 mesh, 1 ml). High-aspect ratio PTFE shrink-tube columns

Step	Resin bed volume equivalent	Reagent
1) Cleaning		
1.1)	4 × 2.5	1 mol l^{-1} NH_4NO_3 – 1 mol l^{-1} NH_4OH
1.2)	2 × 1.5	H_2O
1.3)	4 × 2.5	2 mol l^{-1} HNO_3 – 1 mol l^{-1} HF
1.4)	2 × 1.5	H_2O
2) Condition	3 × 1	3 mol l^{-1} HCl
3) Load sample	5 × 1	3 mol l^{-1} HCl – 0.05 mol l^{-1} HAsc[1]
4) Rinse matrix		
4.1)	3 × 1	3 mol l^{-1} HCl
4.2)	3 × 1	0.5 mol l^{-1} HCl – 0.5% H_2O_2
	2 × 5	0.5 mol l^{-1} HCl – 0. 5% H_2O_2
5) Collect Mo	1 × 8	2 mol l^{-1} HNO_3

[1] HAsc: ascorbic acid.

solution containing Mo was dried down and the residue treated with 0.05 ml of 15 mol l^{-1} HNO_3 and 0.05 ml of 30% *m/m* H_2O_2 to destroy any organic matter introduced during the anionic exchange chemistry (mainly material from disintegrating resin beads occasionally leaking through the polypropylene frit material). After evaporating to dryness the HNO_3–H_2O_2 mixture, the samples were re-dissolved in 0.4 mol l^{-1} HNO_3 – 0.4 mol l^{-1} HF for mass spectrometric analysis.

Several months into the project, we replaced the high-aspect ratio PTFE shrink tube columns by BioRad 'Poly-Prep' low-aspect ratio PP columns with *ca.* 1 cm inner diameter (*ca.* 1.3 cm resin bed height) and filled with 1 ml of AG1x8 (100–200 mesh). While this new set-up (procedure 2) resulted in a two-fold reduction in processing time, we also found an insufficient extraction of Zn. To quantitatively remove Zn while taking advantage of the reduced running time of the new column set-up, a 1 mol l^{-1} HF solution was passed through the columns before Mo was collected in 1 mol l^{-1} HCl (Table 2). Again, after drying down, the Mo cut was treated with a mixture of 0.05 ml 15 mol l^{-1} HNO_3 and 0.05 ml 30% *m/m* H_2O_2 before re-dissolution in 0.4 mol l^{-1} HNO_3 – 0.4 mol l^{-1} HF for mass spectrometric analysis.

For samples with Mo concentrations much lower than 100 ng g^{-1}, such as in the case of USGS BIR-1, *ca.* 1 g of sample material was processed through purification procedure 2. In this case, the sample solution was passed over 2 ml of AG1x8 (100–200 mesh) resin bed volume and acid volumes were adjusted accordingly (see Table 2).

Table 2.
Separation procedure 2 on strongly anionic exchange resin (Bio-Rad and Eichrom AG 1x8, 100 –200 mesh, 1 ml). Low-aspect ratio Bio-Rad 'Poly-Prep' columns

Step	Resin bed volume equivalent	Reagent
1) Cleaning		
1.1)	4 × 2.5	1 mol l^{-1} NH_4NO_3 – 1 mol l^{-1} NH_4OH
1.2)	2 × 1.5	H_2O
1.3)	4 × 2.5	2 mol l^{-1} HNO_3 – 1 mol l^{-1} HF
1.4)	2 × 1.5	H_2O
2) Condition	3 × 1	3 mol l^{-1} HCl
3) Load sample	5 × 1	3 mol l^{-1} HCl – 0.05 mol l^{-1} HAsc[1]
4) Rinse matrix		
4.1)	3 × 1	3 mol l^{-1} HCl
4.2)	3 × 1	0.5 mol l^{-1} HCl – 0.5% H_2O_2
	2 × 5	0.5 mol l^{-1} HCl – 0.5% H_2O_2
4.3)	1 × 10	1 mol l^{-1} HF
4.4)	1 × 3	H_2O
5) Collect Mo	1 × 12	1 mol l^{-1} HCl

[1] HAsc: ascorbic acid.

Mass spectrometric analysis

Instrument equipment and set-up

Isotope ratios of Mo were determined on a ThermoFinnigan Neptune MC-ICP-MS (serial number 1020) at the University of Bristol in 'low-resolution' mode. The instrument is equipped with nine Faraday cups to feedback amplifiers with 10^{11} Ω resistors and 50-V digital voltmeters resulting in a maximum beam current of 5 × 10^{-10} A. The operational settings of the mass spectrometric source are given in Table 3. A dry plasma set-up was used with the sample solution being introduced into the mass spectrometer via a Cetac Aridus desolvating system (Table 3) equipped with a 50 µl min^{-1} micro-concentric PFA nebuliser (Elemental Scientific Ltd.). We found that bleeding small amounts of N_2 into the sample gas flow resulted in an up to two-fold increase of sensitivity and a suppression of oxide formation. All gas flow settings (Table 3) were adjusted on a daily basis to yield maximum sensitivity and signal stability.

Standard nickel sampler and skimmer 'h' cones were used. This set-up gave an average (total) sensitivity of *ca.* 2.5 × 10^{-9} A for a 1 µg ml^{-1} Mo solution. The use of high performance-type cones (i.e., 'x-type' skimmer cones) resulted in an up to fivefold increase of sensitivity but also in unacceptable levels of interferences on masses 96, 94 and 98 of up to several 10^{-12} A. Detailed scans using the high-resolution mode of the ThermoFinnigan Neptune instrument

Table 3.
Typical instrument settings of ThermoFinnigan Neptune MC-ICP-MS during analysis

Parameter	Setting	Parameter		Setting
RF power	1300 W	Sample cone		Ni standard
Reflected power	< 5 W	Skimmer cone		Ni 'h-type'
Cool gas	15 l min^{-1}	Nebuliser	PFA, concentric	50 µl min^{-1}
Auxiliary gas	0.8 l min^{-1}	Aridus	Ar sweep gas	5.5 l min^{-1}
Sample gas	1.0 l min^{-1}		N_2	5 ml min^{-1}
Extraction voltage	2000 V			

when equipped with x-type skimmer cones revealed that these interferences were caused by polyatomic ions $^{40}Ar_2{}^{16}O$, $^{40}Ar_2{}^{14}N$ and $^{40}Ar_2{}^{18}O$ (Table 4). The formation of polyatomic ions appears to be linked to the intrinsic geometry of the high-sensitivity cones. The highest contribution from these interferences was observed when the system was fully optimised to maximum signal intensity. Similar observations have been made for the Nd isotope system when using MC-ICP-MS instruments equipped with high-sensitivity cones (e.g., Newman *et al.* 2009, Newman 2012). Therefore, we refrained from using high-sensitivity cones for the analyses carried out as part of this study.

Pre-sequence checks

After the set-up of the cup configuration (Table 4) and optimisation of the instrument settings (Table 3) for maximum Mo sensitivity, the signals of $^{40}Ar_2{}^{16}O$ and $^{40}Ar_2{}^{14}N$ were monitored by measuring a 0.4 mol l^{-1} HNO_3 – 0.4 mol l^{-1} HF blank solution and checked to be < 10^{-15} A. The $^{40}Ar_2{}^{16}O$ and $^{40}Ar_2{}^{14}N$ interferences have the highest abundance of all Ar_2O and Ar_2N polyatomic ions, and this procedure ensured that all di-argon-oxides and -nitrides were well below detection limits. This was followed by an amplifier gain calibration as well as a six-minute measurement of an electronic baseline with a deflected beam. These factors were used to correct all subsequent measurements (acid blanks, sample–spike mixtures and reference solutions) performed on each day. Before each measurement session, the concentration of sample solutions was adjusted to match the ^{98}Mo signal of the 400 ng ml^{-1} bracketing 'CPI Mo reference solution' (prepared from a 1000 µg ml^{-1} mono-elemental Mo ICP-MS reference solution purchased from CPI International) to within 10% peak height. Only for samples with very low Mo content (i.e., USGS BIR-1), the concentration in the bracketing reference solution was slightly adjusted accordingly. To ensure that the instrument set-up was operating according to our specifications, all sessions were preceded by the measurement of three aliquots of our in-house CPI Mo reference solution mixed with the ^{97}Mo–^{100}Mo double spike. The reference solution/spike ratios ranged from 2:1 to 1:2 by mass and enabled us to assess the effect of variable sample/spike ratio on the accuracy of the determined Mo isotope ratios. For a spiked sample, ion currents for ^{100}Mo and ^{95}Mo typically were *ca.* 3×10^{-10} A and 1.2×10^{-10} A, respectively.

Measurement protocol

Samples were analysed in a sequential and fully automated mode using a Cetac ASX-100 autosampler. The start of each measurement was delayed by 90 s to allow the sample to be fully aspirated and ion signals to stabilise. Usually, *ca.* 0.25 ml of sample solution was consumed during one measurement corresponding to *ca.* 100 ng of Mo. The CPI Mo reference solution (400 ng ml^{-1}, see Archer and Vance 2008) was measured as a bracketing reference solution before and after each sample using the identical measurement conditions (sample take-up time, integration time, number of scans) as a sample/spike mixture (Table 4). Each measurement of a bracketing reference or a sample solution was preceded by a four-min washout period (0.4 mol l^{-1} HNO_3 – 0.4 mol l^{-1} HF solution contained in a 'wash' autosampler vial) followed by a measurement of an 0.4 mol l^{-1} HNO_3 – 0.4 mol l^{-1} HF solution from a separate 'blank' autosampler vial (15 scans of 4 s duration each). The same HNO_3–HF solution mix was used to prepare the reference and sample solutions. This procedure allows the determination of the acid blank and also ensures that cross-contamination between samples and

Table 4.
Cup configuration of ThermoFinnigan Neptune MC-ICP-MS, possible interferences and measurement conditions

Faraday cup	L4	L3	L2	L1	C	H1	H2	H3	H4
Monitored mass	^{90}Zr	^{91}Zr	^{94}Mo	^{95}Mo	^{96}Mo	^{97}Mo	^{98}Mo	^{99}Ru	^{100}Mo
Interfering isotopes			^{94}Zr		^{96}Zr, ^{96}Ru		^{98}Ru		^{100}Ru
Major interfering species			$^{40}Ar_2{}^{14}N$	$^{40}Ar_2{}^{15}N$	$^{40}Ar_2{}^{16}O$	$^{40}Ar_2{}^{17}O$	$^{40}Ar_2{}^{18}O$		
Integration time (in s)	4	4	4	4	4	4	4	4	4
No. of scans	30	30	30	30	30	30	30	30	30

bracketing reference solutions due to protracted wash-out can, if at all present, be identified. Generally, the ion intensities of ^{96}Mo measured in the acid blanks were of the order of 10^{-15} A resulting in a conservative estimate of signal/background ratio of better than *ca.* 150000.

Data reduction and results

The raw intensity data for sample/spike mixtures, reference solutions and acid blank measurements were exported from the ThermoFinnigan Neptune software and further reduced off-line using a ^{95}Mo–^{97}Mo–^{98}Mo–^{100}Mo double-spike inversion implemented into a MATLAB script. Firstly, the average intensities of the solution blank measured before and after each reference solution and sample measurement were subtracted. From these corrected ion intensities, raw isotope ratios ^{97}Mo/^{95}Mo, ^{98}Mo/^{95}Mo and ^{100}Mo/^{95}Mo were calculated. Mass ^{99}Ru was continuously monitored during mass spectrometric analyses (Table 4) and, although no significant levels of Ru were identified in the analyses of this study, a Ru interference correction on Mo masses ^{96}Mo, ^{98}Mo and ^{100}Mo was included to account for any potential minor residual interferences. However, monitored Ru/Mo and Zr/Mo ratios throughout this study were generally below 3×10^{-5} and were found to be negligible.

To account for small differences in instrumental conditions, and hence drift in absolute ratios between the time when the ^{97}Mo–^{100}Mo spike was calibrated relative to the in-house CPI Mo reference solution (Archer and Vance 2008) and the time of the sample/spike mixture measurements of this study, the measured ratios were first re-normalised to the averages of the bracketing CPI Mo reference solutions. The time interval between two measurements of bracketing reference solution, including the measured sample, is short (about 15 min), and thus, a linear interpolation between the two bracketing standards was assumed. Our final deconvolution calculations of the sample/spike mixtures were based on the equations described in Rudge *et al.* (2009). The inversion itself involves the simultaneous solution of three nonlinear equations for three unknowns, that is, the relative proportion of the double spike in the spike–sample mixture, the mass fractionation occurring in the instrument during measurement of the spike–sample mixture and the natural fractionation factor relative to the normalising reference solution. The sample–spike mixing ratios from the inversion were then used to calculate the Mo concentrations of the samples, using sample and tracer weights measured at the beginning of the procedure.

The mass-dependent isotope variations here are reported in the delta notation as parts-per-thousand relative to a reference solution ($\delta^{98}Mo = [(^{98}Mo/^{95}Mo)_{sample}/(^{98}Mo/^{95}Mo)_{reference\ solution}) -1] \times 1000$). To make our results comparable with those from other laboratories, we cross-calibrated our in-house CPI Mo reference solution (Archer and Vance 2008) with NIST SRM 3134 by repeated measurements over the course of the study. NIST SRM 3134 is a Mo concentration reference material and widely used as a commonly available isotopic reference solution (Greber *et al.* 2012, Goldberg *et al.* 2013). However, we do not follow the procedure suggested by Nägler *et al.* (2014) of off-setting the NIST SRM 3134 reference scale to maintain compatibility with earlier δ^{98}Mo values referenced to various reference solutions with slight isotopic differences, such as our CPI Mo reference solution (Archer and Vance 2008). Relative to NIST SRM 3134, we obtained $\delta^{98}Mo = -0.23 \pm 0.01$ (2SE, $n = 42$) for our whole CPI Mo reference solution data set. All δ^{98}Mo values for geological and steel reference materials are reported relative to NIST SRM 3134 in Table 5 using this conversion factor.

Discussion

Matrix separation using a single-step anionic exchange column chemistry

When isolating Mo from silicate matrices, two elements – Fe and Ti – are of particular interest. Both elements occur at % *m/m*-levels in the samples of interest and potentially behave similarly to Mo during most chromatographic separation procedures. Previous studies used a cationic exchange column step to separate Mo from major matrix elements (Barling *et al.* 2001, Burkhardt *et al.* 2014). In this case, Fe weakly partitions on the cationic exchange resin, whereas Mo is not retained. However, an additional column step is then required to further separate Mo from other elements with a preference for forming anionic species in acidic solutions, such as Zr, Ti, Nb. Alternatively, a mixture of 0.5 mol l^{-1} HCl – 1 mol l^{-1} HF may be used as the main eluent on strongly anionic exchange resin (Pearce *et al.* 2009). When loading in a mixture of low-molarity HCl and HF, Fe is not retained on the resin owing to the low partition coefficient of trivalent Fe at low molarity of HCl (Kraus and Nelson 1956). At the same time, Ti is strongly retained on the resin in the presence of HF (Münker *et al.* 2001, Leya *et al.* 2007), leading to a possible saturation of the resin when Ti-rich and Mo-depleted samples are processed.

Several previous studies described a method, in which the samples are loaded in a 7 mol l^{-1} HCl solution with traces of H_2O_2 (Maréchal *et al.* 1999, Archer and Vance 2004, 2008). In such a medium, Ti is not retained on the resin, but Fe is quantitatively oxidised to the trivalent state in

Table 5.
Molybdenum isotope compositions and concentrations of geological and isotopic reference materials

Sample	Type	Distributor	*N*[1]	Mo (mg g^{-1})	2*s*	δ^{98}Mo measured[2]	2*s*	δ^{98}Mo blank corrected[3]	2*s*	Separation procedure
BHVO-2	Basalt	USGS[5]	48	4.2	1.8	-0.07	0.04	-0.07	0.04	1 and 2
AGV-2	Andesite	USGS	3	1.96	0.05	-0.15	0.01	-0.15	0.01	2
BIR-1	Basalt	USGS	3	0.032	0.005	-0.11	0.03	-0.12	0.03	2
JB-2	Basalt	GSJ[6]	4	0.92	0.03	0.05	0.03	0.05	0.03	2
LP-32b[4]	Basalt	University of Bristol	12	4.30	0.05	-0.36	0.04	-0.36	0.04	2
NIST SRM 361	Steel	NIST	21	2008	167	-0.13	0.03	-0.13	0.03	1
Kyoto JMC	Solution	Johnson-Matthey	5	1019	0.3	-0.37	0.01	–[9]	–[9]	–[9]
CPI Mo reference solution[7]	Solution	CPI International	42	–[8]	–[8]	-0.23	0.04	–[9]	–[9]	–[9]

[1] Number of analyses.
[2] Relative to NIST SRM 3134.
[3] Using average procedural blanks processed with respective samples. Uncertainties propagated through the corrections.
[4] In-house reference material.
[5] US Geological Survey.
[6] Geological Survey of Japan.
[7] Prepared from 1000 μg ml^{-1} CPI International Mo concentration solution reference material.
[8] Not determined.
[9] Not processed through column chemistry.

GEOSTANDARDS and GEOANALYTICAL RESEARCH

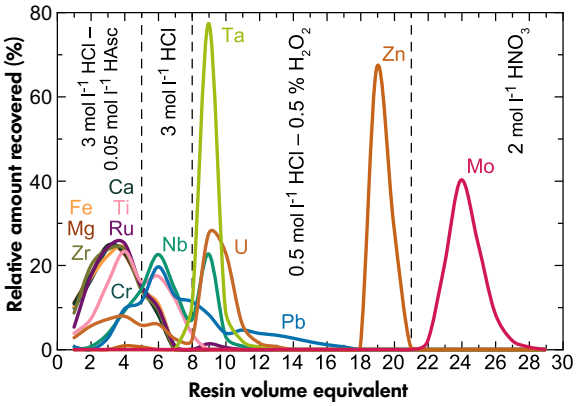

Figure 1. Schematic elution curves for selected major and trace elements using basaltic sample LP-32b and employing separation procedure 1. HAsc: ascorbic acid. See Table 1 and text for discussion.

the presence of H_2O_2 and thus strongly retained on the anionic exchange resin (Kraus and Nelson 1956). As such, this method can only be used for Mo-rich samples with a high Mo/Fe ratio such as sediments (Archer and Vance 2008). It also requires a second clean-up column to eliminate traces of Fe (Archer and Vance 2004).

In this study, silicate samples were processed with Mo concentrations ranging between tens and hundreds of ng g^{-1} and low Mo/Fe, Mo/Ti ratios. At the same time, we aimed to maximise sample throughput as well as to minimise the operator workload and the volume of anionic exchange resin required to process a sample. We therefore chose to design a single-column chemistry that circumvents the above complications. Loading is carried out in 3 mol l^{-1} HCl – 0.05 mol l^{-1} L-ascorbic acid. Under these conditions, Fe^{3+} is reduced to Fe^{2+} by the presence of ascorbic acid (e.g., Pin *et al.* 2014) and thus not retained on the anionic exchange resin (Kraus and Nelson 1956). At the same time, the loading solution does not contain HF, and thus, Ti is efficiently eluted during the loading step. Figure 1 shows a typical elution curve for selected major and trace element using our in-house reference material LP-32b. This sample is an alkaline oceanic basalt from La Palma comprising relatively elevated concentrations of incompatible elements such as Mo. Notably, most elements are either not retained on the AG1x8 resin when loading in 3 mol l^{-1} HCl – 0.05 mol l^{-1} ascorbic acid or are quantitatively washed off the resin in the following 3 mol l^{-1} HCl washing step. Some elements, such as Nb, Ta, Pb, U and Zn, are still present on the resin after rinsing it with 3 mol l^{-1} HCl (Figure 1). We found that Nb, Ta, Pb and U can be quantitatively removed in 0.5 mol l^{-1} HCl – 0.5% H_2O_2 while retaining Mo on the resin. In this case, H_2O_2 acts as a complexing agent that prevents Mo from hydrolysing on the column, comparable to the function of HF in HCl – HF mixtures (Kraus *et al.* 1955, Pearce *et al.* 2009). A similar observation was made when using H_2O_2 as a complexing agent of Ti in a HNO_3 – acetic acid mixture (Münker *et al.* 2001). Figure 1 shows that elimination of remaining matrix elements is achieved when washing the resin with a few column volume equivalents of 0.5 mol l^{-1} HCl – 0.5% H_2O_2 (step 4.2 in Table 1).

Using the high-aspect ratio columns of protocol 1, matrix elements are quantitatively separated from Mo. However, after switching to the low-aspect ratio BioRad 'Poly-Prep' columns, we observed an incomplete separation of Zn from Mo when applying the elution scheme shown in Table 1. We concluded that this protracted elution of Zn was due to the inherent low-aspect column geometry causing a pronounce tailing of the elution peak of Zn. The latter lead to the occasional and spurious formation of a $^{64}Zn^{35}Cl$ interference on mass 99, which was measured to monitor ^{99}Ru during mass spectrometric analyses. To efficiently eliminate Zn from the Mo fraction, we included an additional short washing step in protocol 2 using a 1 mol l^{-1} HF solution followed by a H_2O step to wash out any remaining HF from the resin (steps 4.3 and 4.4 in Table 2). Under these conditions, Mo is strongly retained on the anionic exchange resin (Kraus *et al.* 1955) while any remaining traces of Zn are quantitatively removed.

Cleaning procedure of resin and procedural blank

As detailed in Tables 1 and 2, the resin is cleaned before loading the samples using a combination of alkaline and acidic reagents (step 1). We found that, as an oxy-anionic complex, Mo is strongly retained on anionic exchange resins in acid media. At the same time, MoO_3 precipitates at room temperature at pH < 1 (Greenwood and Earshaw 1997) but is highly soluble in alkaline media. To avoid cross-contamination of Mo still retained on the resin from previous usage of the columns (either as oxy-anionic complex or as precipitates), we rinsed the resin with a mixture of 2 mol l^{-1} NH_4NO_3 – 2 mol l^{-1} NH_4OH in an aqueous solution. Under these alkaline conditions, AG1x8 has a high retention factor of NO_3^-, which efficiently displaces traces of Mo oxy-anionic complexes and dissolves any MoO_3 precipitates still present. After washing out the alkaline solution with H_2O, the cleaning procedure further included a conventional cleaning step using 2 mol l^{-1} HNO_3 – 1 mol l^{-1} HF. Again, Mo and 'high field-strength elements' are not retained on the resin in a HNO_3–HF medium.

The procedural blank of our method was assessed by processing the same quantities of acids through our

procedure as would be used for a regular sample. Several tests were performed using resin previously used to process rock samples and yielded blank contributions ranging between 40 and 600 pg for 1 ml of AG1x8 (100–200) of resin bed volume. We found that acid mixtures comprising HF are prone to contain elevated levels of blank Mo. For this reason, we chose to use a dilute HCl–H_2O_2 mixture to wash out the majority of remaining matrix elements from the resin (see above and step 4.2 in Tables 1 and 2) and only used small amounts of dilute HF and H_2O to remove Zn before collecting Mo using procedure 2 (steps 4.3 and 4.4 in Table 2). Note that the molarity of HCl in the HCl–H_2O_2 mixture was very low and, although the total volume of acid used in this cleaning step was large, its effect on the total procedural blank of the method set-up was negligible. Using this set-up, the contribution of reagents used for sample dissolution and chemical purification to the blank was small – *ca.* 2 pg – with the majority of blank contributed by the resin. We tested different batches of AG1x8 (100–200) resins (BioRad and Eichrom) and found variable procedural Mo blanks from 40 to up to 800 pg Mo. While the above blank contamination had no effect on the δ^{98}Mo of Mo-rich samples, minor corrections were necessary for the Mo-depleted sample USGS BIR-1 (Table 5). Nevertheless, the blank-corrected value of USGS BIR-1 is well within the uncertainty of the measured value (Table 5) and consistent with previous findings (Burkhardt *et al.* 2014).

Recovery of Mo after chemical separation and time consumption

The double-spike approach adopted here allows the simultaneous assessment of a sample's Mo concentration and the amount of Mo recovered after chemical separation. The latter is determined by comparing the measured ^{95}Mo signal in the sample solution and the bracketing reference solutions taking into account the dilution factors as well as the sample mass. Throughout the study, a yield of ~ 95% for both column procedures was observed for a range of silicate and metal reference materials analysed as part of this study. Analyses of a wider range of previously uncharacterised oceanic basalts yielded a similar result. We speculate that a recovery of < 100% is due to the formation of small amounts of insoluble MoO_3 precipitates following the dry-down of the Mo fraction after column chemistry. A similar observation was made during the chemical isolation of W (Willbold *et al.* 2011) and Mo (Burkhardt *et al.* 2014). Nevertheless, we note that a near-quantitative recovery of Mo can be achieved using the anionic exchange method described here.

Methods previously described for the chemical isolation of Mo from geological matrices (Maréchal *et al.* 1999, Barling *et al.* 2001, Archer and Vance 2004, 2008, Pearce *et al.* 2009, Burkhardt *et al.* 2014, Voegelin *et al.* 2014, Greber *et al.* 2015) involve significant amounts of effort and durations in excess of 24 hrs. The present method significantly reduces the time required for the isolation of Mo from matrix elements. From our experience, the purification procedure 2 described here can be completed in > 6 hrs – from sample dissolution in 3 mol l^{-1} HCl – 0.05 mol l^{-1} ascorbic acid to the collection of the pure Mo cut – and therefore provides a significant reduction in sample preparation time.

Imperfect sample–spike ratio and intermediate precision

While we aimed for a 1:1 sample/spike mass ratio for measuring samples (Archer and Vance 2008), imperfect sample/spike mixtures inevitably occurred when measuring unknown samples with unknown Mo concentrations. To assess the robustness of imperfect mixtures on the accuracy of determined δ^{98}Mo values, we measured mixtures of our in-house CPI Mo reference solution and the ^{97}Mo–^{100}Mo spike that ranged between 2:1 and 1:2. Note that sample/spike ratios for samples processed as part of this study (geological reference materials as well as geological samples) all ranged well within these set limits. The results of these measurements (n = 42) are shown in Figure 2, and their average is given in Table 5. The data agree to within 0.04‰ δ^{98}Mo (2s). The latter value also serves as an estimate of the intermediate precision of δ^{98}Mo data over a

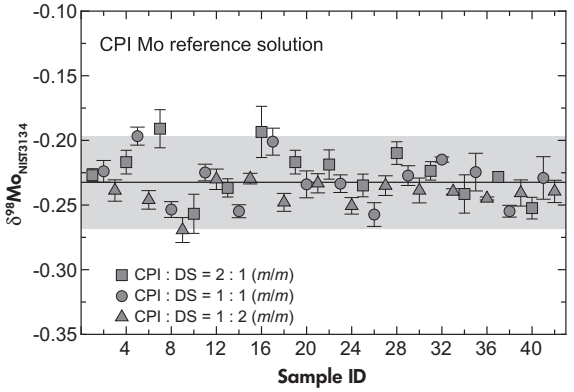

Figure 2. Average value and variations of δ^{98}Mo in our in-house CPI Mo reference solution. Grey bar represents the 2*s* variation of the data set. Note that data for different reference solution (CPI) – double spike (DS) mixtures – agree within 0.04‰ δ^{98}Mo (2*s*). We use this value as an estimate of the intermediate precision of our analytical set-up.

period of *ca.* 2 years using the set-up described here. Our average value for the CPI Mo reference solution was δ^{98}Mo = -0.23 and in very good agreement with recent results ('BIG-Mo', δ^{98}Mo = -0.26 ± 0.05; 2*s*) of an interlaboratory study (Goldberg *et al.* 2013).

Comparison between separation procedures 1 and 2 and data for reference materials

Our intermediate precision of δ^{98}Mo 0.04‰ (2*s*; *n* = 42) based on repeated measurements of the CPI Mo reference solution (Table 5) is comparable to the overall reproducibility of a natural sample such as our basaltic in-house reference material LP-32b (2*s* = 0.04‰ δ^{98}Mo; *n* = 12; Table 5). Our average δ^{98}Mo value obtained for USGS basaltic reference material BHVO-2 (-0.07 ± 0.04‰; 2*s*; *n* = 48) is consistent with that recently published by Burkhardt *et al.* (2014) and is about two times more precise than the value published by Pearce *et al.* (2009), although detailed comparison for this reference material may be compromised by its intrinsic sample heterogeneity, as we discuss below. Aliquots of BHVO-2 were processed through both types of separation procedures (Tables 1, 2 and 5), and data for individual analyses are shown in Figure 3. Average δ^{98}Mo for BHVO-2 using both procedures yielded near identical results (Procedure 1: -0.07 ± 0.04‰; 2*s*; Procedure 2: δ^{98}Mo = -0.06 ± 0.05‰; 2*s*), demonstrating that no systematic error was introduced when changing the analytical set-up.

We have deconvolved our BHVO-2 data with and without applying a Ru correction using the raw data as outlined above. Both approaches yielded identical δ^{98}Mo values and intermediate precision. We are therefore satisfied that interferences of ^{96}Ru, ^{98}Ru and ^{100}Ru on Mo or interferences on mass 99 that would lead to spurious Ru interference corrections are insignificant for the purpose of this study. The Mo concentrations measured in several aliquots of BHVO-2 ranges considerably between *ca.* 2.4 and 6.0 μg g^{-1} with an average of ~ 4.2 μg g^{-1} (Table 5). This is in line with previous findings (Burkhardt *et al.* 2014, Li *et al.* 2014, Yang *et al.* 2015). A plot of δ^{98}Mo values in BHVO-2 versus the inverse of Mo concentrations (Figure 4) shows a weak negative trend suggesting that BHVO-2 powder is heterogeneous on a sampling scale of *ca.* 50–100 mg of rock powder in terms of concentration and isotopic composition. However, the contaminant must have a similar δ^{98}Mo to the natural sample to generate such a shallow slope in Figure 4. Preliminary data for Hawaiian basalts (Willbold, unpublished data; sample powders prepared using metal-free tools) suggest an average concentration of *ca.* 0.3–0.5 μg g^{-1}. Assuming a similar concentration range for the starting material of BHVO-2 (i.e., before industrial-scale milling by the USGS), we suggest that the Mo isotopic composition and concentration of BHVO-2 is dominated by a high Mo component most likely introduced during the bulk preparation of the rock powder. This contamination must be fairly well mixed with the original basaltic rock material although significant heterogeneities persist at the sampling scale and Mo concentration precision levels of this study. Given the siderophile character of Mo and the high Mo concentrations in some industrial steel tools, abraded material from the equipment used to homogenise large amounts of original rock material could represent the source of Mo contamination. Contamination

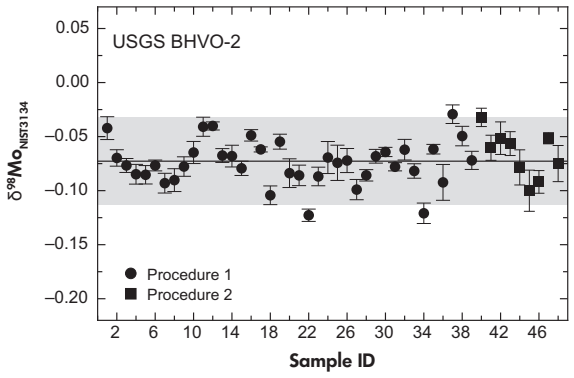

Figure 3. Average value and variations of δ^{98}Mo in basaltic reference material USGS BHVO-2. Line represents average value (δ^{98}Mo = -0.07‰) and grey bar the 2*s* (0.04‰) of the data set. Note that Mo was isolated from the sample matrix using two different procedures. See text for further explanation and discussion.

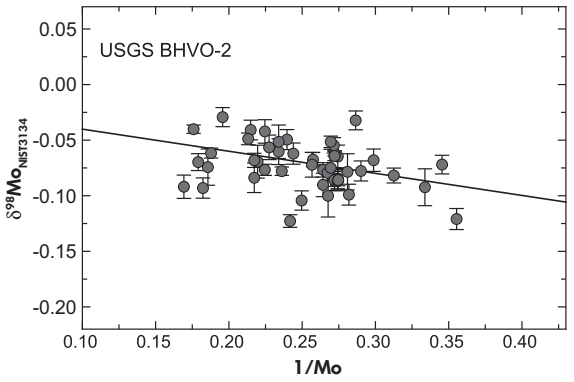

Figure 4. δ^{98}Mo values in BHVO-2 plotted against the inverse of Mo concentration (in μg g^{-1}). Straight line is a simple linear regression through the data set. Error bars represent 2SE of individual measurements. See text for discussion.

during preparation of the BHVO-2 powder has been suggested previously to explain the highly variable Pb concentration in BHVO-2 (Willbold and Jochum 2005) as well as the significantly distinct Pb isotopic composition between both generations of reference materials, BHVO-1 and BHVO-2 (Woodhead and Hergt 2000, Baker *et al.* 2004, Jochum *et al.* 2005, Weis *et al.* 2005). A similar case was made by comparing Mo concentrations of 0.986 and 0.912 μg g^{-1} in BHVO-1 obtained by isotope dilution ICP-MS methods (Makishima and Nakamura 1999, Lu *et al.* 2006) with much higher values in the range of *ca.* 4 μg g^{-1} obtained by double-spike MC-ICP-MS for BHVO-2 (Pearce *et al.* 2009, Babechuk *et al.* 2010, Burkhardt *et al.* 2014).

We note that the intermediate precision as well as the absolute value of δ^{98}Mo in the basaltic USGS reference material BIR-1 (-0.12 ± 0.03‰; Table 5) are nearly identical to the values obtained by Burkhardt *et al.* (2014). Despite the very low concentration of Mo in BIR-1 (0.032 ± 0.005 μg g^{-1}; 2*s*), the intermediate precision of δ^{98}Mo is comparable to that of other Mo-rich reference materials. This demonstrates that our new chemical preparation method and the one employed by Burkhardt *et al.* (2014) are capable of processing large amounts of rock material necessary to achieve such a good reproducibility. At the same time, we stress that our procedure only requires a single chromatographic pass. It shows that, while maintaining a high level of data quality, our method significantly reduces time and effort required to produce highly reproducible and accurate results. Our concentration for BIR-1 is significantly lower than the value of 0.07 ± 0.02 μg g^{-1} obtained by Wieser and DeLaeter (2000). However, we note that the method employed by Wieser and DeLaeter (2000) required correction for procedural blanks in the order of 10 ng Mo, which may compromise the accuracy of Mo concentrations for low-Mo samples. In contrast, our value for BIR-1 is consistent with that of Burkhardt *et al.* (2014) obtained by double-spike MC-ICP-MS (0.032 μg g^{-1}).

We also provide the first Mo isotope data for the andesitic USGS geological reference material AGV-2 and the basaltic Geological Survey of Japan reference material JB-2. Both samples contain intermediate levels of Mo (1.96 ± 0.05 and 0.92 ± 0.03 μg g^{-1}; 2*s*, respectively; Table 5). The δ^{98}Mo value of AGV-2, -0.15 ± 0.01‰ (2*s*), is similar to that of BIR-1 and BHVO-2. In contrast, JB-2 is the only sample of our set of reference materials that displays a small positive δ^{98}Mo offset of +0.05 ± 0.03‰ (2*s*). Over the course of this study, we have routinely measured basalt LP-32b as an in-house reference material (Figure 5). This sample is a historic basanite that erupted in 1712 on La Palma, Canary Islands (Elliott 1991). It displays a significant offset to lower δ^{98}Mo (-0.36 ± 0.04‰; 2*s*; Table 5) and a high, but uniform Mo concentration of 4.30 ± 0.05 μg g^{-1} (2*s*), in keeping with it being an alkali basalt formed by low-degree mantle melting. Overall, the magmatic silicate materials analysed in this study display a narrow range in δ^{98}Mo from -0.36 to +0.05‰. We tentatively assume this range to be representative of rocks originating from subduction zone and mantle recycling processes that is well resolved at the level of reproducibility achieved (2*s* of better than 0.04‰ δ^{98}Mo).

NIST SRM 361 has a δ^{98}Mo value of -0.13 ± 0.03‰ (2*s*; Figure 6) and high levels of Mo (2008 ± 167 μg g^{-1}; 2*s*). Note that NIST SRM 361 also displays a rather large range in measured Mo concentrations. Nevertheless, our

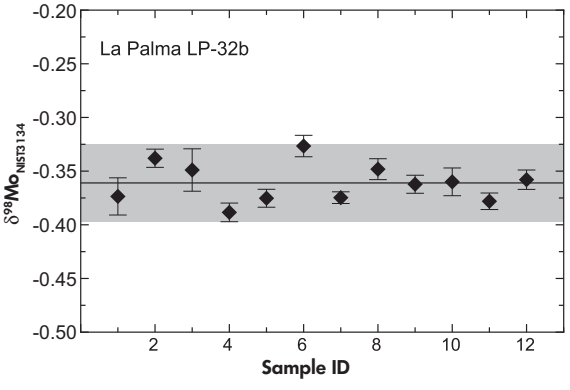

Figure 5. Average value and variations of δ^{98}Mo in La Palma basalt LP-32b used as an in-house reference material. Line represents average value (δ^{98}Mo = -0.36‰) and grey bar the 2*s* (0.04‰) variation of the data set.

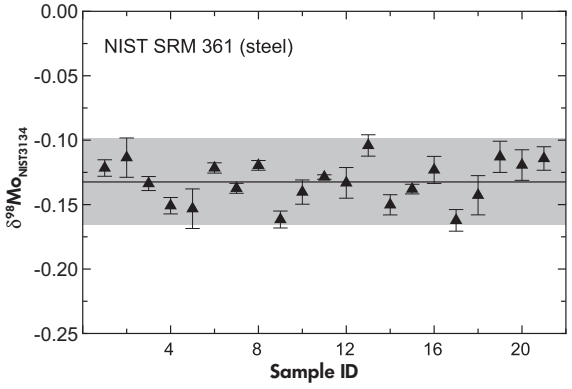

Figure 6. Average value and variations of δ^{98}Mo in NIST SRM 361 (steel). Line represents average value (δ^{98}Mo = -0.13‰) and grey bar the 2*s* (0.03‰) variation of the data set.

average Mo concentration for NIST SRM 361 is within the range of the certified value (1900 ± 100 μg g^{-1}, May and Trahey 2001). However, we speculate that the range in Mo concentration is due to a variable distribution of Mo within the steel. Although we did not determine other element concentrations in NIST SRM 361, we note that some, such as Cu, Co or Mn, also have large uncertainties at the 10% (2*s*) level (May and Trahey 2001). We therefore suggest that NIST SRM 361 may not be homogeneous at the sampling scale of this study.

Our sample set also includes an aliquot of the Kyoto JMC Mo reference solution, for which we obtained a δ^{98}Mo value of -0.37 ± 0.01; 2*s* (Table 5). This value is in excellent agreement with the δ^{98}Mo value of -0.37 ± 0.06 (2*s*) obtained in a recent interlaboratory study (Goldberg *et al.* 2013) and confirms the notion that different batches of in-house JMC Mo reference solutions display significant variations and off-sets to NIST SRM 3134 standards (see Goldberg *et al.* 2013).

Conclusions

The chemical purification method presented here allows quantitative isolation of Mo from matrix elements for a wide range of sample materials including low-concentration silicate samples and Fe-rich metal samples. In particular, the combination of a strongly anionic exchange resin with a loading solution comprising a mixture of HCl and ascorbic acids allows sample sizes in excess of 200 mg to be processed. This makes the method ideally suited to the handling of silicate samples with low Mo concentrations such as basalts and andesites. The data quality of our method is comparable to more complex procedures (Burkhardt *et al.* 2014) even when low-Mo samples are processed. When compared with recent standard techniques for silicate matrices, the reproducibility of δ^{98}Mo data is improved by at least a factor of two (Siebert *et al.* 2003, Wille *et al.* 2007, Pearce *et al.* 2009, Scheiderich *et al.* 2010a, Voegelin *et al.* 2012, Burkhardt *et al.* 2014, Li *et al.* 2014, Voegelin *et al.* 2014, Greber *et al.* 2015) likely largely due to the capability of our method to process larger sample sizes, which allows the samples to be analysed at larger ion intensities. Processing larger sample sizes may also mitigate problems related to the potentially heterogeneous distribution of Mo within the rock sample although this critically depends on the length-scale of sample heterogeneity. Our δ^{98}Mo value for the CPI Mo reference solution and Kyoto JMC Mo compares favourably with values determined in a recent interlaboratory study (Goldberg *et al.* 2013) and confirm that our analytical set-up is able to determine Mo isotope ratios with low uncertainty.

Overall, the purification technique described here is more efficient and less time-consuming when compared with previous methods allowing a higher sample throughput while maintaining a high level of data quality. We therefore suggest that our method is fit-for-purpose to identify small but systematic differences in the mass-dependent Mo isotope variation of mantle-derived rocks.

Acknowledgements

This work greatly benefitted from discussions with C. Archer and D. Vance as well as from their generous sharing of their double-spike and data reduction protocols. This work was made possible by grants from NERC to MW (NE/J018031/1, -/2 and NE/L004011/1) and TE (NE/D012805/1, NE/H023933/1, NE/J009024/1 and NE/J009024/1), which are gratefully acknowledged. HF was supported by a University of Bristol Postgraduate Research Scholarship. We thank two anonymous reviewers for constructive comments that helped to improve the manuscript as well as W. McDonough and T. Meisel for editorial handling.

References

Anbar A.D. (2004)
Molybdenum stable isotopes: Observations, interpretations and directions. **Reviews in Mineralogy and Geochemistry, 55**, 429–454.

Archer C. and Vance D. (2004)
Mass discrimination correction in multiple-collector plasma source mass spectrometry: An example using Cu and Zn isotopes. **Journal of Analytical Atomic Spectrometry, 19**, 656–665.

Archer C. and Vance D. (2008)
The isotopic signature of the global riverine molybdenum flux and anoxia in the ancient oceans. **Nature Geoscience, 1**, 597–600.

Babechuk M.G., Kamber B.S., Greig A., Canil D. and Kodolányi J. (2010)
The behaviour of tungsten during mantle melting revisited with implications for planetary differentiation time scales. **Geochimica et Cosmochimica Acta, 74**, 1448–1470.

Baker J., Peate D.W., Waight T. and Meyzen C. (2004)
Pb isotopic analysis of standards and sample using a ^{207}Pb-^{204}Pb double spike and thallium to correct for mass bias with a double-focussing MC-ICP-MS. **Chemical Geology, 211**, 275–303.

Barling J. and Anbar A.D. (2004)
Molybdenum isotope fractionation during adsorption by manganese oxides. **Earth and Planetary Science Letters, 217**, 315–329.

references

Barling J., Arnold G.L. and Anbar A.D. (2001)
Natural mass-dependent variations in the isotopic composition of molybdenum. **Earth and Planetary Science Letters, 193**, 447–457.

Becker H. and Walker R.J. (2003)
Efficient mixing of the solar nebula from uniform Mo isotopic composition of meteorites. **Nature, 425**, 152–155.

Burkhardt C., Hin R.C., Kleine T. and Bourdon B. (2014)
Evidence for Mo isotope fractionation in the solar nebula and during planetary differentiation. **Earth and Planetary Science Letters, 391**, 201–211.

Dauphas N., Reisberg L. and Marty B. (2001)
Solvent extraction, ion chromatography, and mass spectrometry of molybdenum isotopes. **Analytical Chemistry, 73**, 2613–2616.

Elliott T. (1991)
Element fractionation in the petrogenesis of ocean island basalts. PhD thesis **Open University (UK)**.

Emerson S.R. and Huested S.S. (1991)
Ocean anoxia and the concentrations of molybdenum and vanadium in seawater. **Marine Chemistry, 34**, 177–196.

Freymuth H., Vils F., Willbold M., Taylor R.N. and Elliot T. (2015)
Molybdenum mobility and isotopic fractionation during subduction at the Mariana arc. **Earth and Planetary Science Letters, 432**, 176–186.

Goldberg T., Archer C., Vance D., Thamdrup B., McAnena A. and Poulton S.W. (2012)
Controls on Mo isotope fractionations in a Mn-rich anoxic marine sediment, Gullmar Fjord, Sweden. **Chemical Geology, 296–297**, 73–82.

Goldberg T., Gordon G., Izon G., Archer C., Pearce C.R., McManus J., Anbar A.D. and Rehkämper M. (2013)
Resolution of inter-laboratory discrepancies in Mo isotope data: An intercalibration. **Journal of Analytical Atomic Spectrometry, 28**, 724–735.

Gordon G.W., Lyons T.W., Arnold G.L., Roe J., Sageman B.B. and Anbar A.D. (2009)
When do black shales tell molybdenum isotope tales? **Geology, 37**, 535–538.

Greber N.D., Siebert C., Nägler T.F. and Pettke T. (2012)
$\delta^{98/95}$Mo values and molybdenum concentration data for NIST SRM 610, 612 and 3134: Towards a common protocol for reporting Mo data. **Geostandards and Geoanalytical Research, 36**, 291–300.

Greber N.D., Pettke T. and Nägler T.F. (2014)
Magmatic-hydrothermal molybdenum isotope fractionation and its relevance to the igneous crustal signature. **Lithos, 190–191**, 104–110.

Greber N.D., Puchtel I.S., Nägler T.F. and Mezger K. (2015)
Komatiites constrain molybdenum isotope composition of the Earth's mantle. **Earth and Planetary Science Letters, 421**, 129–138.

Greenwood N.N. and Earshaw A. (1997)
Chemistry of the elements. **Pergamon Press (Oxford)**, 1542pp.

Helz G.R., Miller C.V., Charnock J.M., Mosselmann J.F.W., Pattrick R.A.D., Garner C.D. and Vaughan D.J. (1996)
Mechanism of molybdenum removal from the sea and its concentration in black shales: EXAFS evidence. **Geochimica et Cosmochimica Acta, 60**, 3631–3642.

Jochum K.P., Pfänder J., Woodhead J.D., Willbold M., Stoll B., Herwig K., Amini M., Abouchami W. and Hofmann A.W. (2005)
MPI-DING glasses: New geological reference materials for *in situ* Pb isotope analysis. **Geochemistry Geophysics Geosystems, 6**, doi:10.1029/2005GC000995.

Kraus K.A. and Nelson F. (1956)
Anion-exchange studies of the fission products. **United Nations International Conference on the Peaceful Uses of Atomic Energy, 7**, 113–125.

Kraus K.A., Nelson F. and Moore G.E. (1955)
Anion-exchange studies. XVII. Molybdenum (VI), tungsten (VI) and uranium (VI) in HCl and HCl-HF solutions. **Journal of the American Chemical Society, 77**, 3972–3977.

Leya I., Schönbächler M., Wiechert U., Krähenbühl U. and Halliday A.N. (2007)
High precision titanium isotope measurements on geological samples by high resolution MC-ICP-MS. **International Journal of Mass Spectrometry, 262**, 247–255.

Li J., Liang X.-R., Zhong L.-F., Wang X.-C., Ren Z.-Y., Sun S.-L., Zhang Z.-F. and Xu J.-F. (2014)
Measurement of the isotopic composition of molybdenum in geological samples by MC-ICP-MS using a novel chromatographic extraction technique. **Geostandards and Geoanalytical Research, 38**, 345–354.

Lu Y., Makishima A. and Nakamura E. (2006)
Coprecipitation of Ti, Mo, Sn and Sb with fluorides and application to determination of B, Ti, Zr, Nb, Mo, Sn, Sb, Hf and Ta by ICP-MS. **Chemical Geology, 236**, 13–26.

Makishima A. and Nakamura E. (1999)
Determination of molybdenum, antimony and tungsten at sub μg g^{-1} levels in geological materials by ID-FI-ICP-MS. **Geostandards Newsletter: The Journal of Geostandards and Geoanalysis, 23**, 137–148.

Maréchal C.N., Télouk P. and Albarède F. (1999)
Precise analysis of copper and zinc isotopic compositions by plasma-source mass spectrometry. **Chemical Geology, 156**, 251–273.

references

May W.E. and Trahey N.M. (2001)
National Institute of Standards & Technology Certificate of Analysis, Standard Reference Material 361.

McManus J., Nägler T.F., Siebert C., Wheat C.G. and Hammond D.E. (2002)
Oceanic molybdenum isotope fractionation: Diagenesis and hydrothermal ridge-flank alteration. Geochemistry Geophysics Geosystems, 3, doi:10.1029/2002GC000356.

Münker C., Weyer S., Scherer E. and Mezger K. (2001)
Separation of high field-strength elements (Nb, Ta, Zr, Hf) and Lu from rock samples for MC-ICP-MS measurements. Geochemistry Geophysics Geosystems, 2, doi:10.1029/2001GC000183.

Nagai Y. and Yokoyama T. (2014)
Chemical separation of Mo and W from terrestrial and extraterrestrial samples via anion exchange chromatography. Analytical Chemistry, 86, 4856–4863.

Nägler T.F., Anbar A.D., Archer C., Goldberg T., Gordon G.W., Greber N.D., Siebert C., Sohrin Y. and Vance D. (2014)
Proposal for an international molybdenum isotope measurement standard and data representation. Geostandards and Geoanalytical Research, 38, 149–151.

Newman K. (2012)
Effects of the sampling interface in MC-ICP-MS: Relative elemental sensitivities and non-linear mass dependent fractionation of Nd isotopes. Journal of Analytical Atomic Spectrometry, 27, 63–70.

Newman K., Freedman P.A., Williams J., Belshaw N.S. and Halliday A.N. (2009)
High sensitivity skimmers and non-linear mass dependent fractionation in ICP-MS. Journal of Analytical Atomic Spectrometry, 24, 742–751.

Pearce C.R., Cohen A.S., Coe A.L. and Burton K.W. (2008)
Molybdenum isotope evidence for global ocean anoxia coupled with perturbations to the carbon cycle during the Early Jurassic. Geology, 36, 231.

Pearce C.R., Cohen A.S. and Parkinson I.J. (2009)
Quantitative separation of molybdenum and rhenium from geological materials for isotopic determination by MC-ICP-MS. Geostandards and Geoanalytical Research, 33, 219–229.

Pin C., Gannoun A. and Dupont A. (2014)
Rapid, simultaneous separation of Sr, Pb, and Nd by extraction chromatography prior to isotope ratios determination by TIMS and MC-ICP-MS. Journal of Analytical Atomic Spectrometry, 29, 1858–1870.

Rudge J.F., Reynolds B.C. and Bourdon B. (2009)
The double spike toolbox. Chemical Geology, 265, 420–431.

Scheiderich K., Helz G.R. and Walker R.J. (2010a)
Century-long record of Mo isotopic composition in sediments of a seasonally anoxic estuary (Chesapeake Bay). Earth and Planetary Science Letters, 289, 189–197.

Scheiderich K., Zerkle A.L., Helz G.R., Farquhar J. and Walker R.J. (2010b)
Molybdenum isotope, multiple sulfur isotope, and redox-sensitive element behavior in early Pleistocene Mediterranean sapropels. Chemical Geology, 279, 134–144.

Siebert C., Nägler T.F. and Kramers J.D. (2001)
Determination of molybdenum isotope fractionation by double-spike multicollector inductively coupled mass spectrometry. Geochemistry Geophysics Geosystems, 2, doi:10.1029/2000GC000124.

Siebert C., Nägler T.F., von Blankenburg F. and Kramers J.D. (2003)
Molybdenum isotope records as a potential new proxy for paleoceanography. Earth and Planetary Science Letters, 211, 159–171.

Voegelin A.R., Nägler T.F., Pettke T., Neubert N., Steinmann M., Pourret O. and Villa I.M. (2012)
The impact of igneous bedrock weathering on the Mo isotopic composition of stream waters: Natural samples and laboratory experiments. Geochimica et Cosmochimica Acta, 86, 150–165.

Voegelin A.R., Pettke T., Greber N.D., von Niederhäusern B. and Nägler T.F. (2014)
Magma differentiation fractionates Mo isotope ratios: Evidence from the Kos Plateau Tuff (Aegean Arc). Lithos, 190–191, 440–448.

Wasylenki L.E., Rolfe B.A., Weeks C.L., Spiro T.G. and Anbar A.D. (2008)
Experimental investigation of the effects of temperature and ionic strength on Mo isotope fractionation during adsorption to manganese oxides. Geochimica et Cosmochimica Acta, 72, 5997–6005.

Weis D., Kieffer B., Maerschalk C., Pretorius W. and Barling J. (2005)
High-precision Pb-Sr-Nd-Hf isotopic characterization of USGS BHVO-1 and BHVO-2 reference materials. Geochemistry, Geophysics, Geosystems, 6, doi:10.1029/2004GC000852.

Wieser M.E. and DeLaeter J.R. (2000)
Molybdenum concentrations measured in eleven USGS geochemical reference materials by isotope dilution thermal ionisation mass spectrometry. Geostandards Newsletter: The Journal of Geostandards and Geoanalysis, 24, 275–279.

Willbold M. and Jochum K.P. (2005)
Multi-element isotope dilution sector field ICP-MS: A precise technique for the analysis of geological materials and its application to geological reference materials. Geostandards and Geoanalytical Research, 29, 63–82.

Willbold M., Elliott T. and Moorbath S. (2011)
The tungsten isotopic composition of the Earth's mantle before the terminal bombardment. Nature, 477, 195–198.

Wille M., Kramers J.D., Nägler T.F., Beukes N.J., Schröder S., Meisel T., Lacassie J.P. and Voegelin A.R. (2007)
Evidence for a gradual rise of oxygen between 2.6 and 2.5 Ga from Mo isotopes and Re-PGE signatures in shales. Geochimica et Cosmochimica Acta, 71, 2417–2435.

references

Woodhead J.D. and Hergt J.M. (2000)
Pb-isotope analyses of USGS reference materials. **Geostandards Newsletter: The Journal of Geostandards and Geoanalysis, 24**, 33–38.

Xu L., Lehmann B., Mao J., Nägler T.F., Neubert N., Böttcher M.E. and Escher P. (2012)
Mo isotope and trace element patterns of Lower Cambrian black shales in South China: Multi-proxy constraints on the paleoenvironment. **Chemical Geology, 318–319**, 45–59.

Yang J., Siebert C., Barling J., Savage P., Liang Y.-H. and Halliday A.N. (2015)
Absence of molybdenum isotope fractionation during magmatic differentiation at Hekla volcano, Iceland. **Geochimica et Cosmochimica Acta, 162**, 126–136.

Yin Q., Jacobsen S.B. and Yamashita K. (2002)
Diverse supernova sources of pre-solar material inferred from molybdenum isotopes in meteorites. **Nature, 415**, 881–883.